

Supporting Information

Experimental Section

Materials

Methanol was purchased from Fisher Scientific. Acetaminophen was purchased from MP Biomedicals.

Crystallization

Crystals of the monoclinic form were grown from methanol solutions (100 mg/mL) dissolved at room temperature. Solutions were passed through a syringe filter into a 20 mL vial and colorless block crystals were formed upon evaporation of the solvent at room temperature.

Crystals of the orthorhombic form were grown from DI water solutions (25 mg/mL) heated to 65 °C for 1 hour to dissolve all solids. Solutions were passed through a syringe filter (2 mL) into a 4 mL vial and allowed to cool to room temperature. One vial at a time was placed in a recirculating bath containing a 50:50 mixture of ethylene glycol and water held at 0 °C. After 4 hours, the vial was removed and tapped on the benchtop. This disturbance initiates nucleation, and the vial was placed back in the chiller for another hour. Colorless needles were formed and must be isolated (by pipetting dropwise onto filter paper to remove excess solution quickly) to prevent transformation to the monoclinic polymorph.

Infrared Spectroscopy

Fourier transform infrared spectroscopy experiments were performed on the monoclinic and orthorhombic forms of acetaminophen using an attenuated total reflectance accessory (ATR; ThermoNicolet Avatar model 360-FTIR). The scan range was 680 to 4000 cm^{-1} , employing 512 scans with a resolution of 4 cm^{-1} . Samples were analyzed on the ATR stage and the empty stage was used as the blank.

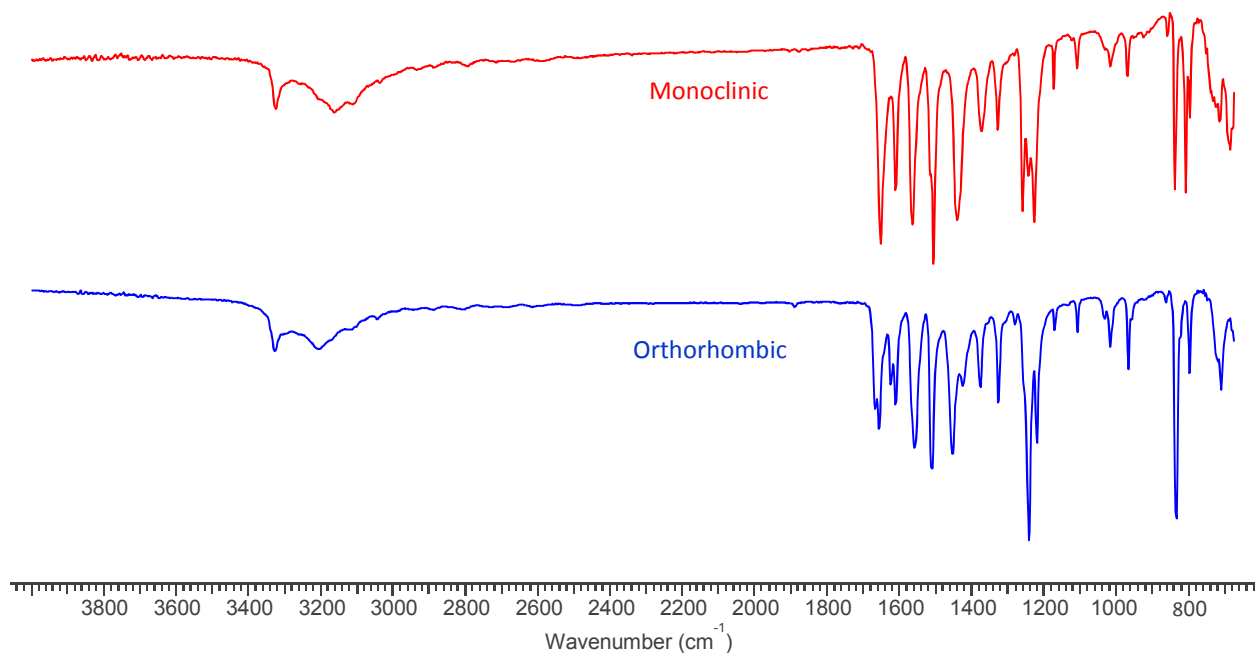


Figure S1. IR spectra of monoclinic (top) and orthorhombic (bottom) forms of acetaminophen.

Raman Spectroscopy

Raman spectra were collected using a Renishaw inVia Raman Microscope equipped with a Leica microscope, 633 nm laser, 1800 lines/mm grating, 50 μm slit, and a RenCam CCD detector. Spectra were collected in extended scan mode with a range of 100-3200 cm^{-1} and then analyzed using the WiRE 3.4 software package (Renishaw). Calibration was performed using a silicon standard.

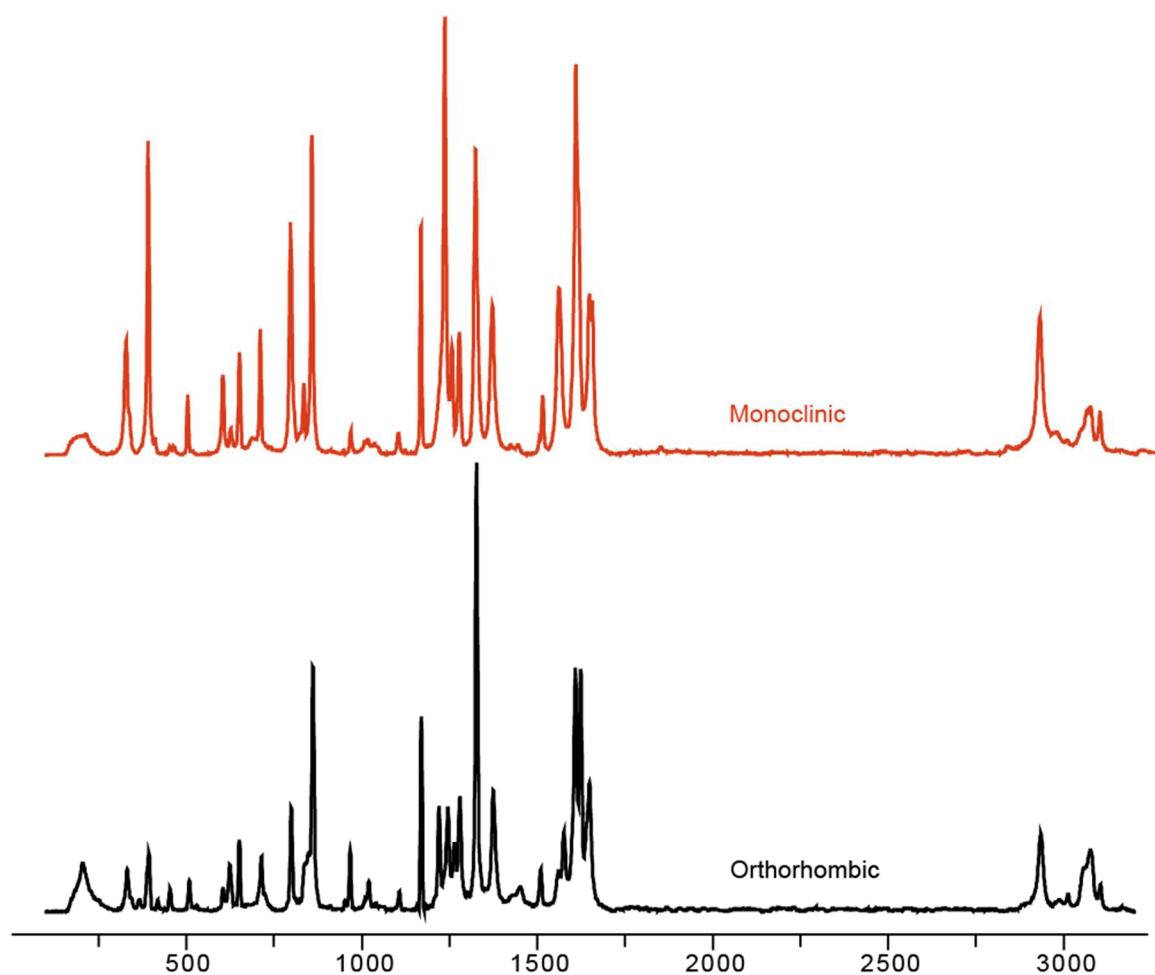


Figure S2. Raman spectra of monoclinic (top) and orthorhombic (bottom) forms of acetaminophen.

Solid-State NMR Spectroscopy. All NMR experiments were conducted at 14.1 T on a 600-MHz JEOL solid-state NMR spectrometer (JEOL ECA600II) operating at ^1H and ^{13}C Larmor frequencies of 600.17 MHz and 150.91 MHz, respectively, using either a 0.75-mm double-resonance Ultrafast MAS probe or a 1.0-mm double-resonance Ultrafast MAS probe (JEOL RESONANCE Inc., Tokyo, Japan). All measurements were carried out at ambient temperature using about one mg of acetaminophen samples packed separately into ultrafast MAS zirconia rotors. One-dimensional (1D) ^1H MAS spectra were

recorded in 3 scans using a rotor-synchronized spin-echo (τ_r -180°- τ_r) pulse sequence with a $\pi/2$ ^1H pulse of 0.8 μs and a recycle delay of 120 s at multiple 90 kHz MAS frequency. The 1D ^{13}C CP MAS NMR spectrum of the orthorhombic acetaminophen was recorded in 416 scans under 70 kHz MAS with a ^1H excitation pulse of 1.5 μs and a recycle delay of 250 s using a ramped-amplitude cross-polarization (Ramp-CP)¹ pulse sequence during an acquisition period of 54 ms with a 2.6 ms cross-polarization contact time. The ^1H -detected ^{13}C - ^1H 2D HETCOR spectrum of the orthorhombic acetaminophen was recorded at 70 kHz MAS with a 1.2 μs $\pi/2$ ^1H pulse using a recycle delay of 140 s and 128 t_1 increments ($t_{1\text{max}} = 3.392$ ms) with 8 scans per increment during a t_2 acquisition time of 20.48 ms. Contact times of 2.6 and 0.5 ms were respectively used for the ^1H to ^{13}C and ^{13}C to ^1H ramped CP steps. The HORROR condition was applied for a duration of 5 ms with 36.15 kHz ^1H RF amplitude to remove all the residual transverse magnetization on protons. The 2D $^1\text{H}/^1\text{H}$ CSA/CS correlation spectra for the monoclinic and orthorhombic forms of acetaminophen were collected using a γ -encoded symmetry-based pulse sequence depicted below $R18_8^7(270^\circ 90^\circ)$ at 90 kHz MAS^{2,3}. $R18_8^7(270^\circ 90^\circ)$ pulse sequence is composed of a series of 270° and 90°- composite 180° recoupling pulses with phases alternating between 70° and 250°, respectively. The NMR data were acquired using an acquisition time of 10.24 ms with 1024 t_2 complex points. Six scans for every t_1 point with a total of 32 t_1 increments were used to obtain the amplitude-modulated signal at every $8\tau_r$ period. Prior to the application of symmetry-based ^1H CSA recoupling pulses, a relaxation delay of 120 s was used for both samples. The decoupled spectra were obtained with ^{14}N - ^1H decoupling (99W/ \sim 117 kHz) using an on-resonance (121 ppm / 5.25 kHz) ^{14}N continuous wave irradiation during the ^1H CSA recoupling t_1 period to avoid the reintroduction of ^{14}N - ^1H dipolar interactions. The ^{14}N shifts (on-resonance conditions) were measured from 2D $^{14}\text{N}/^1\text{H}$ HMQC correlation experiments for both polymorphs. 2D $^1\text{H}/^1\text{H}$ CSA/CS correlation data were processed using Delta NMR software (JEOL RESONANCE Inc., Tokyo, Japan) by applying a Fourier transform after zero-filling in the direct frequency domain. A DC balance (the average of the final 1/8th points of the FID in the t_1 dimension is subtracted from the total data points) prior to zero-filling followed by a real Fourier

transform in the indirect frequency domain to get rid of the DC offset effects that result in a narrow center peak with a significant intensity, which affects the ^1H CSA line shapes through the wiggles originating from this center peak.

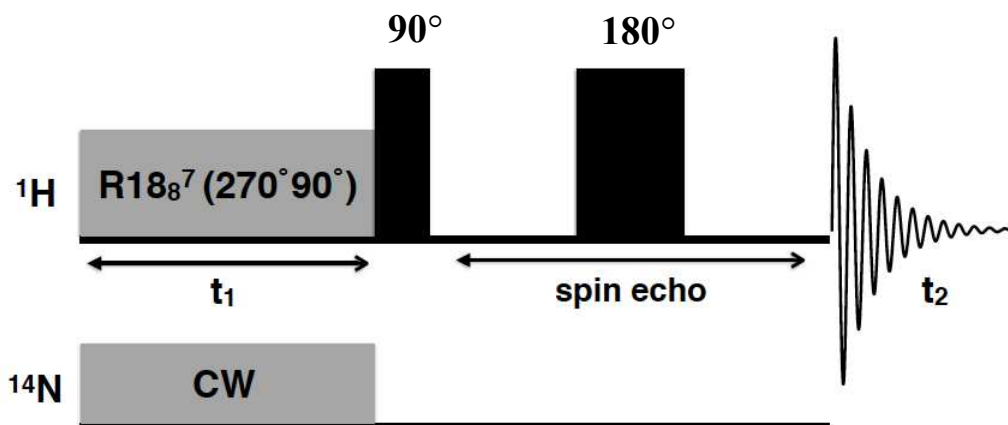


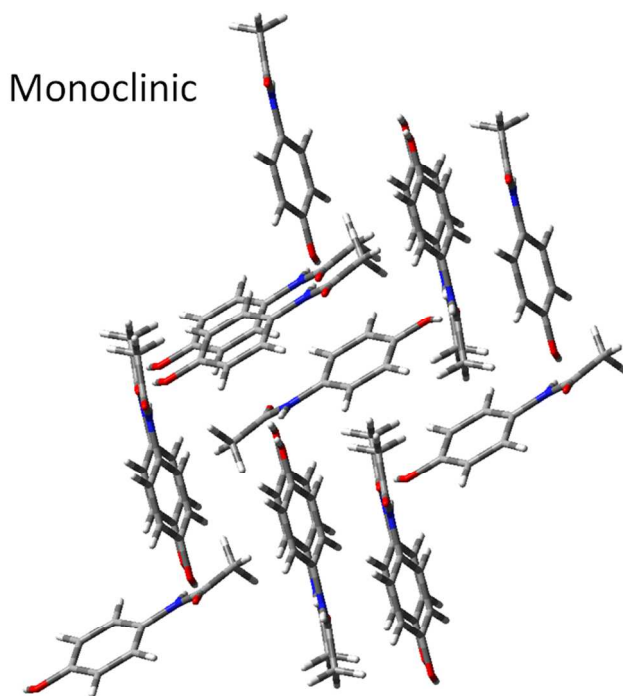
Figure S3. Schematic of the radio-frequency pulse sequence used for all CS/CSA correlations experiments.

NMR Simulation. Numerical simulations using SIMPSON⁴ were carried out for a single ^1H spin system in the absence of RF field inhomogeneity to fit the experimental ^1H CSA line shapes obtained from the spectral slices parallel to the ^1H CSA dimension at ^1H isotropic chemical shift values of monoclinic and orthorhombic forms of acetaminophen. In these simulations, powder averaging was achieved using 678 (α, β) orientations and 26 γ angles at a ^1H Larmor frequency of 600 MHz under 90 kHz MAS by implementing γ -encoded symmetry-based sequence $R18_8^7 (270^\circ 90^\circ)$. To get the best fit, the simulated ^1H CSA line shapes were adjusted by applying a vertical intensity scaling and single exponential line-broadening function.

Computational Details. Quantum chemical calculations were performed using Gaussian 09 program.⁵ Calculations of the ^1H magnetic shielding tensors were carried out on molecular clusters constructed using atomic coordinates from the single-crystal X-ray crystal structure for each polymorph.⁶ For each polymorph, this cluster consists of 15 molecules (a total of 300 atoms), where a central acetaminophen

molecule is surrounded by its nearest neighbors up to a distance of $\sim 15 \text{ \AA}$ (see Figure S4). The hydrogen atom positions were optimized with density functional theory (DFT) using the Becke-Lee-Yang-Parr three-parameter exchange-correlation functional (B3LYP)^{7,8} and the 6-31G(d,p) basis function for all atoms. The proton magnetic shielding tensors were calculated for the optimized structures with DFT at the B3LYP/6-311G(d,p) level for all atoms using the Gauge-Including Atomic Orbital (GIAO) method.^{9,10} The magnetic shielding tensor components of the protons in the central molecule, as calculated in Gaussian 09, were converted to chemical shift tensor components using the isotropic shielding constant of a fully optimized tetramethylsilane (TMS) calculated at the same level of theory:

$$\delta_{ii}^{\text{calc}} = \sigma_{\text{iso}}^{\text{TMS}} - \sigma_{ii}^{\text{calc}}.$$



Orthorhombic

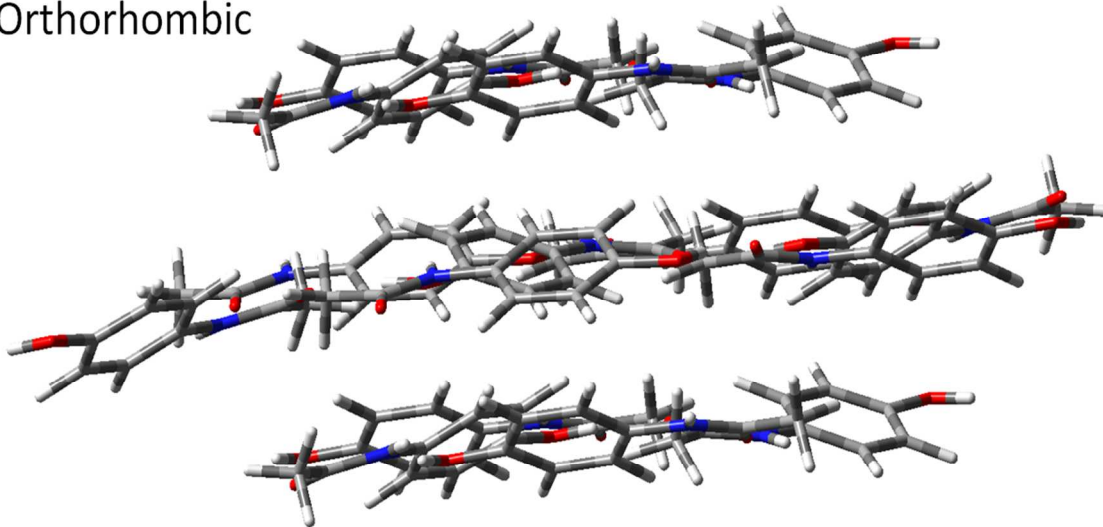


Figure S4. Molecular cluster models used in the calculation of ^1H chemical shielding tensors for the two polymorphs of acetaminophen.

Table S1. The computed ^1H NMR chemical shift parameters (based on the 6-311G(d,p) functional) of the two acetaminophen polymorphs, along with the experimentally measured values. The reported parameters are the isotropic chemical shift δ_{iso} , the CSA (defined as $\zeta = \delta_{\text{zz}} - \delta_{\text{iso}}$), and the asymmetry parameter $\eta = (\delta_{\text{yy}} - \delta_{\text{xx}}) / \zeta$, shift), where the three principal components of the chemical shift tensor are ordered as $|\delta_{\text{zz}} - \delta_{\text{iso}}| \geq |\delta_{\text{xx}} - \delta_{\text{iso}}| \geq |\delta_{\text{yy}} - \delta_{\text{iso}}|$.

Orthorhombic	OH	b	f	c	e	CH₃
Expt. δ_{iso} (ppm)	9.4	7.1	4.7	4.7	6.3	1.8
Expt. $ \zeta $ (ppm)	15.3	6.7	6.3	6.3	5.8	3
Expt. η	0.3	0.6	0.7	0.7	0.75	1
Calc. δ_{iso} (ppm)	9.0	8.2	5.6	5.4	7.3	2.4
Calc. ζ (ppm)	-16.1	6.6	4.2	2.9	-4.0	-3.7
Expt. η	0.6	0.9	1.0	0.7	0.3	0.8
Monoclinic	OH	b	f	c	e	CH₃
Expt. δ_{iso} (ppm)	9.4	8.0	6.8	6.8	5.8	1.1
Expt. $ \zeta $ (ppm)	16.4	7.4	5.6	5.6	4.8	5
Expt. η	0.4	0.6	0.7	0.7	1	1
Calc. δ_{iso} (ppm)	9.0	8.3	7.4	7.6	6.4	1.8
Calc. ζ (ppm)	-14.1	-6.9	4.8	-4.6	-3.9	-5.7
Calc. η	0.4	0.6	1.0	0.9	0.6	0.6

Table S2. The computed ^1H NMR chemical shift anisotropy tensors expressed in standard convention as principal components δ_{zz} , δ_{xx} , and δ_{yy} from both basis sets.

Monoclinic	OH	b	f	c	e	CH₃
δ_{iso} 6-31G(d,p)	9.0	8.1	7.3	7.6	6.5	2.0
δ_{zz} 6-31G(d,p)	19.1	13.7	12.3	12.1	9.5	6.6
δ_{xx} 6-31G(d,p)	13.0	9.3	7.0	7.7	7.2	3.4
δ_{yy} 6-31G(d,p)	-5.1	1.4	2.7	3.0	2.8	-3.9
δ_{iso} 6-311G(d,p)	9.0	8.3	7.4	7.6	6.4	1.8
δ_{zz} 6-311G(d,p)	19.0	13.6	12.1	11.9	9.6	6.3
δ_{xx} 6-311G(d,p)	12.9	9.8	7.3	7.9	7.1	3.0
δ_{yy} 6-311G(d,p)	-4.9	1.4	7.7	2.9	2.5	-3.9
Orthorhombic	OH	b	f	c	e	CH₃
δ_{iso} 6-31G(d,p)	8.8	8.1	7.4	5.6	5.7	2.
δ_{zz} 6-31G(d,p)	21.9	14.8	10.1	8.5	10.0	5.3
δ_{xx} 6-31G(d,p)	12.3	7.5	8.4	5.3	5.1	2.6
δ_{yy} 6-31G(d,p)	-7.7	2.0	3.5	3.0	1.5	-1.9
δ_{iso} 6-311G(d,p)	9.0	8.2	7.3	5.6	5.4	2.7
δ_{zz} 6-311G(d,p)	21.8	14.8	10.0	9.8	8.3	6.0
δ_{xx} 6-311G(d,p)	12.4	7.8	8.7	5.5	4.9	3.2
δ_{yy} 6-311G(d,p)	-7.1	1.9	3.4	1.4	3.0	-1.0

NMR Resonance Assignment

The ^1H and ^{13}C NMR resonance assignments for the monoclinic form were previously reported by Zhou and Rienstra under 40 kHz MAS.¹¹ In a similar fashion, the assignments of proton and carbon resonances in the orthorhombic form can be performed. To this end, we measured the 2D ^1H -detected ^1H - ^{13}C HETCOR NMR spectrum under MAS of 70 kHz for the orthorhombic polymorph as well as the ^1H - ^{13}C cross polarization spectrum, which are shown in Figure S5. Shown also in Figure S5 (A and B) are the 1D ^1H MAS NMR spectra of the two forms under 90 kHz MAS. Figure S5(C and D) shows the assignments of the proton and carbon atoms in the orthorhombic form of acetaminophen. The resonance at 170 ppm in the ^{13}C dimension of the HETCOR spectrum corresponds to the carbonyl carbon, reflected by its strong cross-peak with the methyl protons, which in turn exhibit a cross-peak with the methyl carbon at (2.0, 24.3) ppm. The amide proton is assigned to 9.0 ppm based on its cross-peaks with the carbonyl carbon and the aromatic quaternary carbon *a*, which is in turn assigned to 131 ppm. Based on their cross-peak with carbon *a*, the aromatic protons *b* and *f* are assigned to 7.2 and 4.9 ppm, respectively. The OH proton is assigned to 9.4 ppm as it shares a single cross-peak with the quaternary carbon *d* at (9.4, 152.4) ppm, which in turn shares a cross-peak with protons *c* and *e* at 4.9 and 6.5 ppm. According to the crystal structure of the orthorhombic acetaminophen, the carbonyl group lies closely in the plane of the phenyl group, and therefore is spatially closer to either proton *b* or *f*. From DFT calculations, we confirm that the closest phenyl proton is in fact the most downfield shifted. If we take the orientation of the molecule presented in Figure S5, then proton *b* is the most downfield phenyl proton. Accordingly, the assignment for the phenyl protons would most likely be *b* at 7.2 ppm, *e* at 6.5 ppm, and *c/f* at 4.9 ppm.

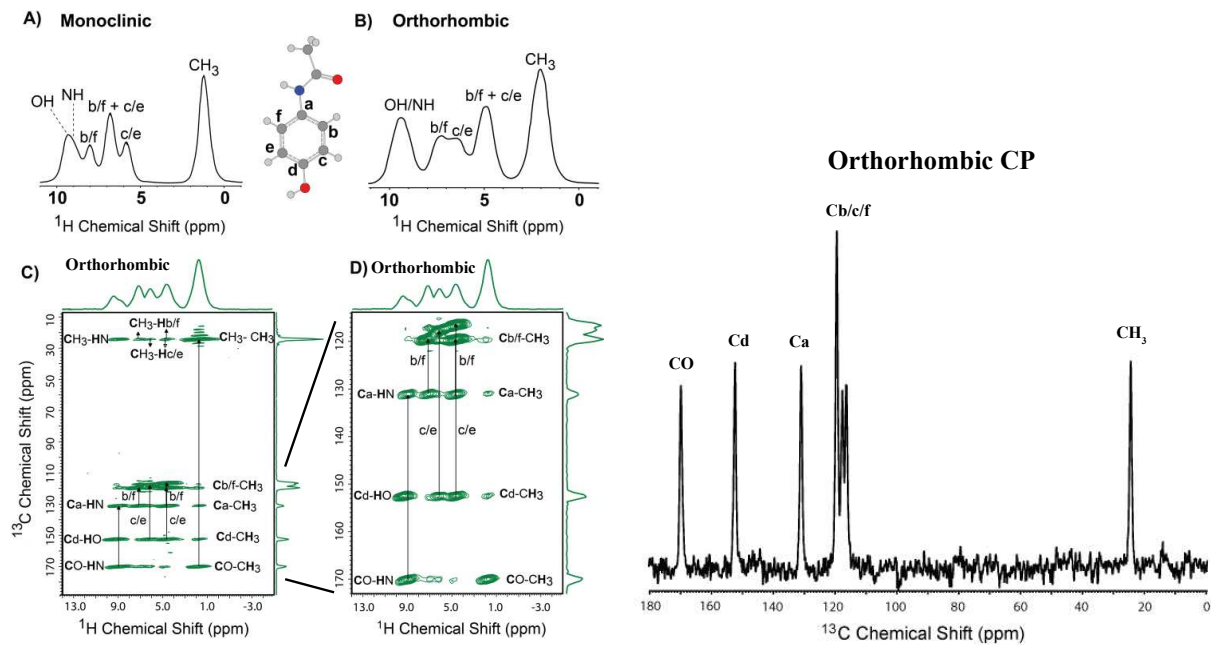


Figure S5: A) and B) ^1H MAS NMR spectra of both polymorphic forms with assignments. C) ^{13}C - ^1H Two-dimensional HETCOR NMR spectrum of orthorhombic and D) the HETCOR spectrum for the aromatic region alone. Right is the normal ^{13}C CPMAS NMR spectrum of the orthorhombic obtained at 70 kHz MAS.

The Role of ^{14}N - ^1H Heteronuclear Dipolar couplings

SIMPSON simulations of the CSA line-shapes were performed including the ^1H - ^{14}N heteronuclear couplings from the nearest neighbor for each resonance and compared to CSA-only line-shapes using the experimentally determined CSA parameters for the orthorhombic (Figure S6) and the monoclinic (Figure S7). The dipolar coupling constants used were computed from the crystal structure based on the static distances between the nuclei. The influence of the heteronuclear couplings, to a greater or lesser extent, causes distortions by smoothing the line-shapes. This is the source of the erroneous CSA fits described in the main text without decoupling. In both polymorphs, the aromatic resonances are more influenced by the inclusion of the couplings in the simulations. Experimentally, however, the influence is found to be more prevalent for the orthorhombic, which we attribute to differing contributions of the molecular dynamics. A more rigid orthorhombic crystal (or more dynamic monoclinic molecule) explains this behavior. It is important to note that the line-shapes below are a simplification given that they do not account for longer range effects of even other close by ^{14}N interactions. As such, they should not reflect the exact line-shape of the experiment but give the general influence of the interaction. A rather broad coupling was found for the NH resonance and shown in the bottom right of Figures S6 and S7 confirming that the satellite peaks in main text are indeed from the NH spin pair.

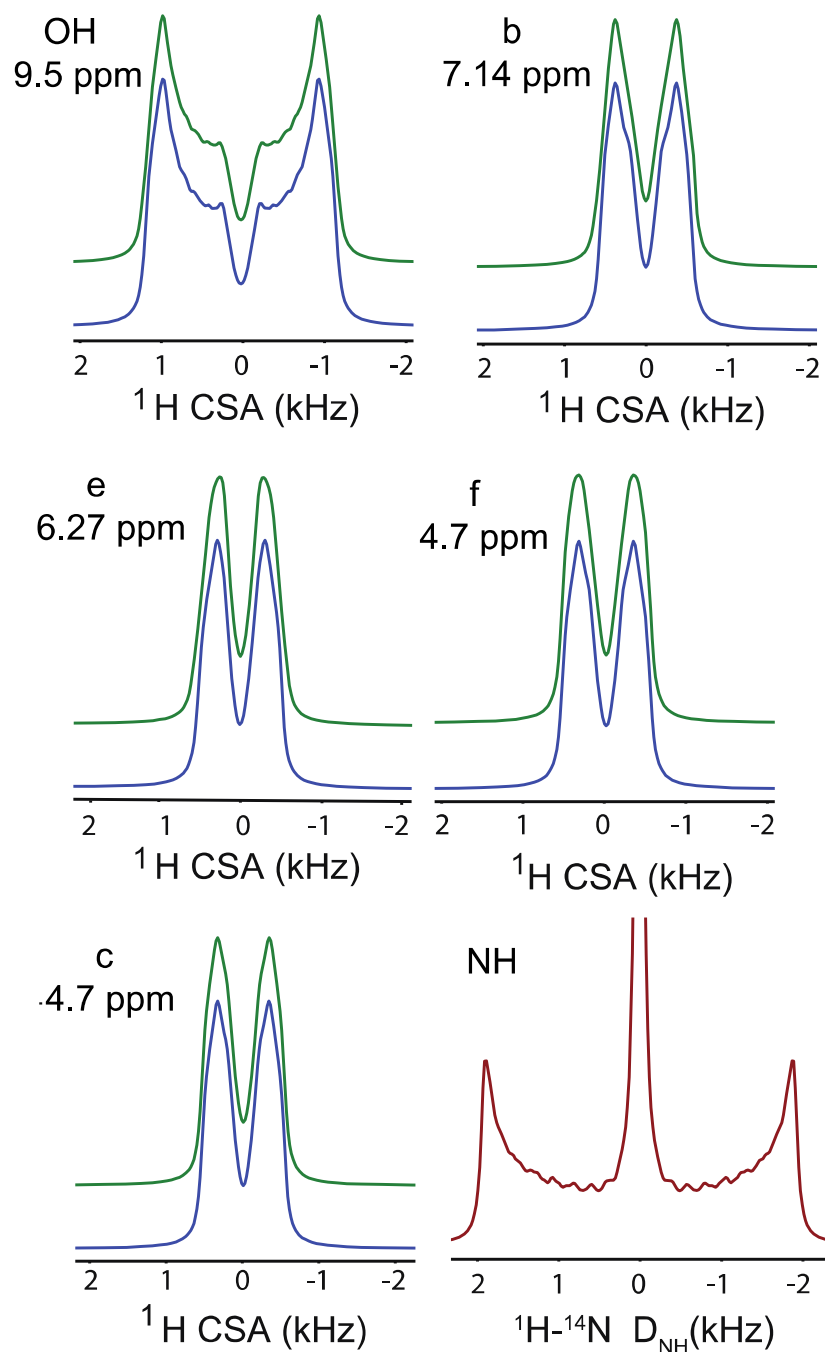


Figure S6. SIMPSON simulations comparing ^1H CSA line-shapes with (green) and without (blue) ^1H - ^{14}N heteronuclear couplings for the orthorhombic polymorph of acetaminophen. The spectrum for the dipolar coupling alone is included in the bottom right for the NH resonance.

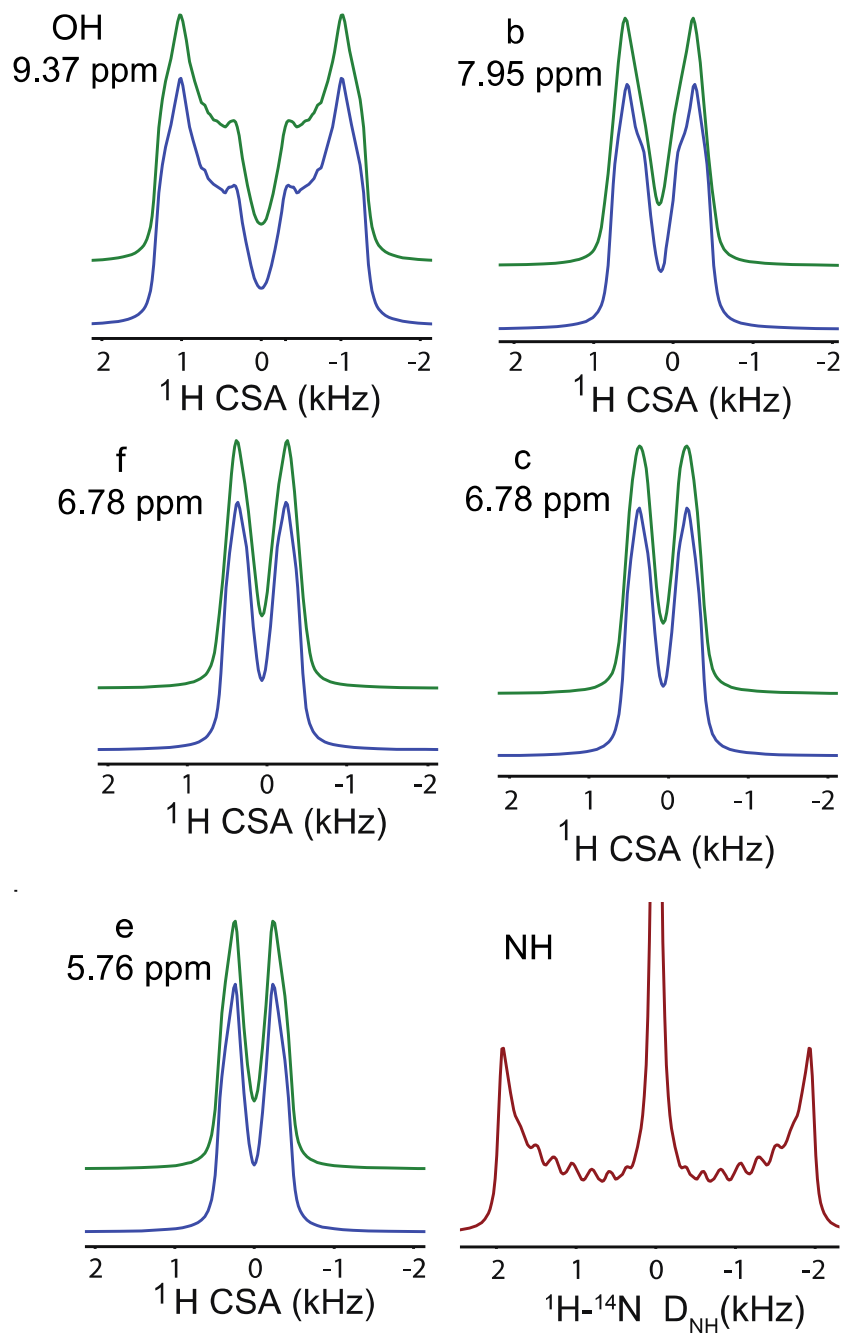


Figure S7. SIMPSON simulations comparing ^1H CSA line-shapes with (green) and without (blue) ^1H - ^{14}N heteronuclear couplings for the monoclinic polymorph of acetaminophen. The spectrum for the dipolar coupling alone is included in the bottom right for the NH resonance.

References

- (1) Metz, G.; Wu, X. L.; Smith, S. O. Ramped-Amplitude Cross Polarization in Magic-Angle-Spinning NMR. *J. Magn. Reson. Ser. A* **1994**, *110*, 219–227.
- (2) Pandey, M. K.; Nishiyama, Y. Determination of NH Proton Chemical Shift Anisotropy with ¹⁴N-¹H Heteronuclear Decoupling Using Ultrafast Magic Angle Spinning Solid-State NMR. *J. Magn. Reson.* **2015**, *261*, 133–140.
- (3) Pandey, M. K.; Malon, M.; Ramamoorthy, A.; Nishiyama, Y. Composite-180° Pulse-Based Symmetry Sequences to Recouple Proton Chemical Shift Anisotropy Tensors under Ultrafast MAS Solid-State NMR Spectroscopy. *J. Magn. Reson.* **2015**, *250*, 45–54.
- (4) Bak, M.; Rasmussen, J. T.; Nielsen, N. C. SIMPSON: A General Simulation Program for Solid-State NMR Spectroscopy. *J. Magn. Reson.* **2000**, *147*, 296–330.
- (5) Frisch, M. J.; Trucks, G. W.; Schlegel, H. B.; Scuseria, G. E.; Robb, M. A.; Cheeseman, J. R.; Scalmani, G.; Barone, V.; Mennucci, B.; Petersson, G. A.; Nakatsuji, H.; Caricato, M.; Li, X.; Hratchian, H. P.; Izmaylov, A. F.; Bloino, J.; Zheng, G.; Sonnenber, D. J. Gaussian 09. *Gaussian, Inc. Wallingford CT* **2009**, 2–3.
- (6) Nichols, G.; Frampton, C. S. Physicochemical Characterization of the Orthorhombic Polymorph of Paracetamol Crystallized from Solution. *J. Pharm. Sci.* **1998**, *87*, 684–693.
- (7) Becke, A. D. Density-functional Thermochemistry. III. The Role of Exact Exchange. *J. Chem. Phys.* **1993**, *98*, 5648–5652.
- (8) Lee, C.; Yang, W.; Parr, R. G. Development of the Colle-Salvetti Correlation-Energy Formula into a Functional of the Electron Density. *Phys. Rev. B* **1988**, *37*, 785–789.
- (9) Ditchfield, R. Self-Consistent Perturbation Theory of Diamagnetism. *Mol. Phys.* **1974**, *27*, 789–807.
- (10) Wolinski, K.; Hinton, J. F.; Pulay, P. Efficient Implementation of the Gauge-Independent Atomic Orbital Method for NMR Chemical Shift Calculations. *J. Am. Chem. Soc.* **1990**, *112*, 8251–8260.

- (11) Zhou, D. H.; Rienstra, C. M. Rapid Analysis of Organic Compounds by Proton-Detected Heteronuclear Correlation NMR Spectroscopy with 40 kHz Magic-Angle Spinning. *Angew. Chemie - Int. Ed.* **2008**, *47*, 7328–7331.